

Available online at www.sciencedirect.com**ScienceDirect**

Procedia Materials Science 10 (2015) 50 – 63

Procedia
Materials Sciencewww.elsevier.com/locate/procedia

2nd International Conference on Nanomaterials and Technologies (CNT 2014)

Investigation of Trapezoidal-Cut Twisted Tape Insert in a Double Pipe U-Tube Heat Exchanger using Al₂O₃/Water Nanofluid

P.V. Durga Prasad^{1,*}, A.V.S.S.K.S. Gupta² and K. Deepak³¹Department of Mechanical Engineering, DRK Institute of Science and Technology, Hyderabad, India²Department of Mechanical Engineering, JNTUH College of Engineering, Hyderabad, India³Department of Mechanical Engineering, Vardhaman College of Engineering, Hyderabad, India

Abstract

An attempt is made to enhance the rate of heat transfer in heat exchangers using Al₂O₃ nanofluid. In this work an experimental analysis on trapezoidal-cut twisted tape insert in a double pipe U-tube heat exchanger using Al₂O₃ water based nanofluid is presented. The heat transfer coefficients and the corresponding friction factors required for performance analysis are determined taking into account the typical operating conditions of the heat exchangers in turbulent flow regimes with particle volume concentration of 0.01% and 0.03% and twist ratios ranging between 5 and 20. Experimental data is generated at flow rates ranging from 0.0333 kg/s to 0.2667 kg/s. Experimental data is generated with water and nanofluid for Reynolds number in the range 3000 < Re < 30000, the Nusselt number of entire pipe for 0.03% concentrations of nanofluid with trapezoidal-cut twisted tape inserts of H/D = 5 is enhanced by 34.24% as compared to water. The friction factor of entire pipes for 0.03% concentration of nanofluid with trapezoidal-cut twisted tape inserts of H/D=5 is enhanced by 1.29 times as compared to water. The results of the investigation indicate an enhancement in the performance parameters of the heat exchanger namely heat transfer coefficient and friction factor with an increase in volume concentration of the nanoparticle.

© 2015 The Authors. Published by Elsevier Ltd. This is an open access article under the CC BY-NC-ND license (<http://creativecommons.org/licenses/by-nc-nd/4.0/>).

Peer-review under responsibility of the International Conference on Nanomaterials and Technologies (CNT 2014)

Keywords: Nanofluid, Heat exchanger, Friction factor, Heat transfer enhancement, Trapezoidal-cut twisted tape inserts.

1. INTRODUCTION

Many heat transfer processes occur in industrial applications in which heat exchangers of various kinds are used. Double pipe heat exchangers are widely used in power plants, chemical plants, food processing, oil and gas industry. The analysis of heat exchanger begins with an energy balance and material balance for any kind of process. Conventional fluids such as water, ethylene glycol and engine oil have relatively low thermal conductivities, when

*Corresponding author. Tel.: + 91 944 043 4220

E-mail address: pvdurgap@gmail.com

compared to the thermal conductivity of solids. Heat transfer of the working fluid can be improved by the thermal conductivity. To increase the thermal conductivity of a fluid, to suspend nano sized solid particles in the fluid to

Nomenclature

A	Area of heat transfer m^2
d_i	Inside tube diameter, m
d_o	Outside tube diameter, m
d_h	Hydraulic diameter, m
H/D	Trapezoidal-cut Twist ratio = Pitch/tube diameter =Y
L	Length of tube
Δp	Pressure drop, Kg/m^2
m	Mass flow rate, kg/s
Q	Rate of heat transfer, W
C_p	Specific heat of fluid, $KJ/kg.K$
T_{hi}, T_{ho}	Inlet and outlet temperature of hot fluid, $^{\circ}C$
T_{ci}, T_{co}	Inlet and outlet temperature of cold fluid, $^{\circ}C$
h_i	Inside heat transfer coefficient , $W/m^2.K$
h_o	Out side heat transfer coefficient, $W/m^2.K$
ΔT_{LMTD}	Log mean temperature difference, K
K	Thermal conductivity of fluid, W/mK
f	Friction factor
U	Overall heat transfer coefficient, $W/m^2.K$

improve heat transfer characteristics of the fluid. Insertion of a twisted tape with trapezoidal - cut section is one such technique applied and investigated to ascertain the enhancement of heat transfer in the double pipe U-tube heat exchanger. One of the methods to enhance the rate of heat transfer is to generate turbulence in the flow.

The dispersion of a low volume (<1%) fraction of solid nanoparticles in traditional base fluid drastically increases the thermal conductivity than that of base fluid Chopkar et al. (2007, 2006). Lee et al. (1999) demonstrated a maximum increase in the thermal conductivity increases maximum 20% when CuO nanoparticles were suspended in ethylene glycol. Suspending copper nanoparticles mean diameter size less than 10 nm, Eastman et al. (2001) was able to increase the thermal conductivity of ethylene glycol up to 40%. Pak and Cho (1998) performed experiments on convective heat transfer of nanofluids under turbulent flow conditions using Al_2O_3 and TiO_2 dispersed in water. Further, enhanced techniques have been discussed in detail by Eiamsa-ard et al. (2006) for experimentally investigating the effect of twisted tape insert on heat transfer in the tube side of a double pipe heat exchanger and also measured the heat transfer without twisted tape. Bergles (1995) Twisted tape techniques have been used to augment heat transfer in double pipe heat exchanger. Dewan et al. (2004), Anil Singh Yadav (2008) investigated heat transfer and the pressure drop characteristics in a double pipe heat exchanger with full length twisted tape inserts. Experimental investigations of heat transfer and friction factor characteristics of circular tube fitted with full length twisted tape with trapezoidal-cut were studied for the Reynolds number range of 2000-12000 by Murugesan et al. (2009) .

The relevant works cited above reveals that good amount of investigations have been carried out on heat exchangers with inserts of various shapes. Keeping view of these earlier works, the aim of the present investigation is mainly on performance analysis of heat exchangers with twisted tape inserts having trapezoidal- cut section with water and water based Al_2O_3 nanofluid with 0.01% and 0.03% volume concentration and Reynolds number range is 3000 to 30000, respectively. The parameters like heat transfer coefficient, friction factor and thermal performance are evaluated and compared with heat exchanger without inserts to ascertain the relative quantum of enhancement of heat transfer rates by using inserts.

2. EXPERIMENTAL SETUP AND PROCEDURE

2.1 Preparation of Nanofluid

The nanofluids for the present study were prepared by dispersing Al₂O₃ nanoparticles in distilled water. The nanoparticles are procured from Sigma-Aldrich Chemicals, USA. The thermal properties of distilled water and the physical properties of Al₂O₃ nanoparticles are reported in **Table 1**.

Table 1 Thermo-physical properties of Al₂O₃ nanoparticles and base fluid.

Particle/Base fluid	Diameter (nm)	Purity (%)	ρ (kg/m ³)	Surface area to mass, (m ² /g)	C (J/kg K)	K (W/m K)
Al ₂ O ₃	< 50 nm	99	3970	29	525	17.65
Distilled water*	$\rho = 1001.67 - 0.10408T - 0.0033T^2$ $C_p = 4192 - 0.70975T + 0.00956T^2$ $\mu = 1.445 \times 10^{-6} - 2.525 \times 10^{-8}T + 1.475 \times 10^{-10}T^2$ $k = 0.55815 + 0.00222T - 1.025 \times 10^{-5}T^2$					

*All temperatures are in degrees Celsius.

To avoid sedimentation of the particles for making stable nanofluids, surfactant is to be added in the base fluid, the best results were obtained with sodium dodecyl benzene sulphate (SDBS) surfactant. The weight of SDBS surfactant used is nearly equal to 1/10th of weight of nanoparticles for a particular concentration; surfactant is prepared by mixing with water and then stirring by using a high speed stirrer. The nanoparticles required for a known volume concentration is estimated from equation given below.

$$\phi = \frac{1}{(100/\phi_m)(\rho_p/\rho_w)^{\phi}} \times 100 (\%) \quad (1)$$

Where (ρ_p) and (ρ_w) are the densities of the particles and water, respectively, (ϕ) and (ϕ_m) are the volume and mass concentrations (%) of the dispersed fluid, respectively.

2.2 Experimental setup and working procedure

The representation of the experimental setup is depicted in **Fig. 1a**, along with its photograph in **Fig. 1b**; it consists of a test section, data logger, personal computer, flow meter, receiving tank, chiller, hot fluid tank, pump, bypass valve arrangement and u-tube manometer. The test section consists of a U-bend double pipe heat exchanger; the inner tube is chromium steel and it has an inner diameter (ID) of 0.019 m, and the annulus tube is made of cast iron with an ID of 0.05 m. The total length of the inner tube is 5m and the bend is equidistant from both ends at a distance of 2.5 m; with radius of 0.160 m. The inner tube is concentric to the annulus tube and fully enclosed by it. The hot fluid is pumped through the annular region and the water/nanofluid flows through the inner tube by using a pump, and are controlled with by-pass valves, the two flow meters are used to measure the mass flow rate of cold fluid and hot fluid. Throughout the experiments the mass flow rate of hot fluid through annulus is kept constant (0.095 kg/s) and the working fluid mass flow rate is varied from 0.033 kg/s to 0.26 kg/s. The test section consists of inlet pipe, bend and outlet pipe as depicted in **Fig. 1a**. The heat transfer coefficients for the inner and outer pipes are calculated; the surface area related to the bend region is relatively small compared to the surface areas of the inner and outer pipes. Therefore, the heat transfer in the bend region can be neglected with no significant loss of accuracy. The outside surface of the annulus tube is wounded with asbestos rope insulation to minimize the heat loss from the test section to atmosphere. In order to measure the temperatures of the fluids, a total of eight K-type thermocouples are used, in which four are located at the inner pipe of the heat exchanger and four at the outer pipe of the heat exchanger. Thermocouple needles are connected to the data acquisition system and the thermocouple readings are

recorded in the computer for further processing. The thermocouples are calibrated ($\pm 0.1\%^\circ\text{C}$) before placing in the test section. The aspect ratio ($l/d=264$, l : length, d : diameter) of the test section is sufficiently high for hydrodynamically developed flow. The nanofluid, which runs in a closed loop, before entering the test section passes through a chiller to maintain the inlet temperature is constant. The pressure drop across the inner tube of the test section is measured by placing a U-tube manometer between both ends of the tube and mercury as the manometric fluid. Once the hot fluid reaches steady state of 70°C , readings of the eight thermocouples are recorded and used for heat transfer calculations. The experimental setup is calibrated with water as the working fluid, prior to using the 0.01% and 0.03% volume concentrations of Al_2O_3 nanofluid. The tube is cleaned with pure water in between the experiments conducted with the nanofluid. The dimensions of the inserts are shown in Table 2.

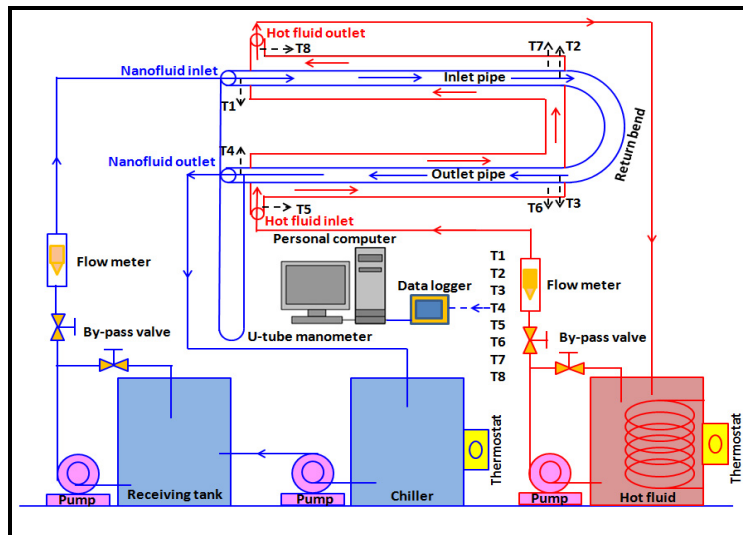


Fig. 1a Schematic diagram of experimental setup



Fig. 1b Photograph of an experimental setup.



Fig. 1c Schematic representation of trapezoidal-cut twisted tape

Table 2 Dimensions of the trapezoidal-cut twisted tape inserts

S. No.	Parameter	Y=Twist Ratio, H/D			
		5	10	15	20
1	H (Pitch)	0.108	0.18	0.27	0.36
2	D (Diameter)	0.018	0.018	0.018	0.018

3. DATA ANALYSIS

3.1 Measurement of thermophysical properties of nanofluids

The thermophysical properties (density, specific heat, viscosity and thermal conductivity) of the nanofluid are calculated as a function of nanoparticle volume concentration together with properties of base fluid and nanoparticles. The density and specific heat of nanofluid are evaluated using the general formula for the mixture:

$$\rho_{nf} = \phi \rho_p + (1 - \phi) \rho_{bf} \quad (2)$$

$$C_{p,nf} = \phi C_{p,p} + (1 - \phi) C_{p,bf} \quad (3)$$

These equations have been found appropriate for nanofluids through experimental validation by Pak and Cho (1998). The thermal conductivity are calculated from Maxwell (1904) as shown in Eq. (4) which is recommended for homogeneous and low volume concentration liquid–solid suspensions with randomly dispersed, uniformly sized and non interacting spherical particles.

$$k_{nf} = k_{bf} \left[\frac{k_p + 2k_{bf} + 2\phi (k_p - k_{bf})}{k_p + 2k_{bf} - \phi (k_p - k_{bf})} \right] \quad (4)$$

Viscosity of nanofluids is calculated with Einstein's formula (1956).

$$\mu_{nf} = \mu_{bf} (1 + 2.5\phi) \quad (5)$$

Where (μ) is the viscosity and the subscripts (*p*), (*bf*) and (*nf*) refer to particle, base fluid and nanofluid, respectively.

3.2 Trapezoidal-Cut Twisted Tapes

The trapezoidal-cut twisted tapes are made of 1.00 mm thick aluminium strips, the width of the strip being 1 mm less than the inside diameter of the test section tube. The strips are twisted on a lathe by manual rotation of the chuck. The twist ratio (*y*) for this strip is defined as the ratio between one length of twist (or) pitch length to diameter. The full length twisted tape has its trapezoidal–cut dimensions as 6 mm deep, 6 mm at its base and 10 mm wide at its top. The trapezoidal-cut is taken alternately on both top and bottom of the tape to improve the fluid mixing near the inner walls of the pipe. The schematic of this trapezoidal cut test section is shown in Fig. 1c

3.3 Heat transfer, friction factor and thermal performance

The experimental data is summarized in the following procedures. Heat transfer to the working fluid (Water/Nanofluid) in the test section, Q_c

$$Q_c = m_c C_{pc} (T_{co} - T_{ci}) \quad (6)$$

Where, m_c is the mass flow rate of cold fluid, C_{pc} is the specific heat of cold fluid; T_{ci} and T_{co} are the cold water inlet and outlet temperatures respectively.

The heat transfer rate of hot water in the annulus side, Q_h

$$Q_h = m_h C_{ph} (T_{hi} - T_{ho}) \quad (7)$$

Here, m_h is the mass flow rate of hot water, $C_{p,h}$ is the specific heat of water, T_{hi} and T_{ho} are the hot fluid inlet and outlet temperatures respectively.

The average heat transfer rate Q_{ave} is estimated from the hot fluid and cold fluid sides is as follows:

$$Q_{avg} = (Q_c + Q_h)/2 \tag{8}$$

Fluid flows in a concentric tube heat exchanger, an overall heat transfer coefficient (U) is calculated from:

$$Q_{avg} = UA_i(\Delta T)_{LMTD} \tag{9}$$

Where $A_i = \pi d_i L$

$$\text{Entire region, } (\Delta T)_{LMTD} = [(T_3 - T_1) - (T_5 - T_3)] / \ln \frac{(T_3 - T_1)}{(T_5 - T_3)} \tag{10}$$

The tube-inside heat transfer coefficient h_i is determined by using

$$1/U_i = 1/h_i + (d_i/k) \ln \frac{d_o}{d_i} + (d_o/d_i) (1/h_o) \tag{11}$$

From Eq. (11) except $1/U_i$ and $1/h_i$ remaining terms are kept constant, the Eq. (11) can be re-written as:

$$\frac{1}{U_i} = \frac{1}{h_i} + Q \tag{12}$$

The heat transfer coefficient is related to Reynolds number as:

$$h_i = C Re^m \tag{13}$$

Substitute Eq. (13) into Eq. (12) yields

$$\frac{1}{U_i} = \frac{1}{C Re^m} + Q = P Re^{-m} + Q \tag{14}$$

Eq. (14) implies that the plot between $1/U_i$ and Re^{-m} is a straight line with its slope of P and intercept at Q in Y-axis ($1/U_i$). Rearranging Eq. (14) can be re-written as proposed in Wongcharee and Eiamsa-ard (2012)

$$h_i = 1/(1/U_i - Q) \tag{15}$$

The average Nusselt number based on the inner diameter of the tube, was then evaluated by

$$Nu = \frac{h_i \times d_i}{k} \tag{16}$$

The Reynolds number is based on the flow rate at the inlet of the tube.

$$Re = \frac{\rho v d_i}{\mu}$$

Where μ is the dynamic viscosity of the working fluid.

Friction factor, f can be calculated from

$$f = \frac{\Delta P}{(L/D)(\rho v^2/2)} \tag{17}$$

Where Δp is the pressure drop across the test section, ρ is the density of working fluid, d_i is the inner diameter of tube, v is the velocity of working fluid, and L is the length of tube.

The thermal performance factor (η) is defined as the ratio of the heat transfer coefficient (or Nusselt number, Nu) ratio to the friction factor (f) ratio at the same pumping power:

$$\eta = (Nu/Nu_p)/(f/f_p)^{1/3} \tag{18}$$

Where Nu_p and f_p are the Nusselt number and friction factor of the plain tube.

4. RESULTS AND DISCUSSION

4.1 Validation of plain tube data

Estimation of Nusselt number and friction factor from the data obtained with working fluid as water, the experimental setup is validated along with the data, Eq. (16) of Gnielinski (1956) and Eq. (21) of Notter-Rouse (1972) and is shown in Fig. 2. The difference between experimental and theoretical Nusselt number for water was obtained a maximum of $\pm 3\%$.

The available Nusselt number correlations for single phase fluid are given below:

- (i) Gnielinski (1956) equation

$$Nu = \frac{(\frac{L}{D})(Re-1000)Pr}{1.07+12.7(\frac{L}{D})^{0.5}(Pr^{2/3}-1)} \tag{19}$$

$$f = (1.58 \ln(Re) - 3.82)^{-2}; 2300 < Re < 10^6; 0.5 < Pr < 2000 ;$$

- (ii) Notter-Rouse (1972) equation

$$Nu = 5 + 0.015Re^{0.856}Pr^{0.347} \tag{20}$$

The available Nusselt number correlations for Al_2O_3 nanofluid is given below:

- (iii) Pak and Cho (1998) equation

$$Nu = 0.021 Re^{0.8} Pr^{0.5} \tag{21}$$

$$0 \le \phi \le 3.0\%; 6.54 \le Pr \le 12.33, 10^4 \le Re \le 10^5$$

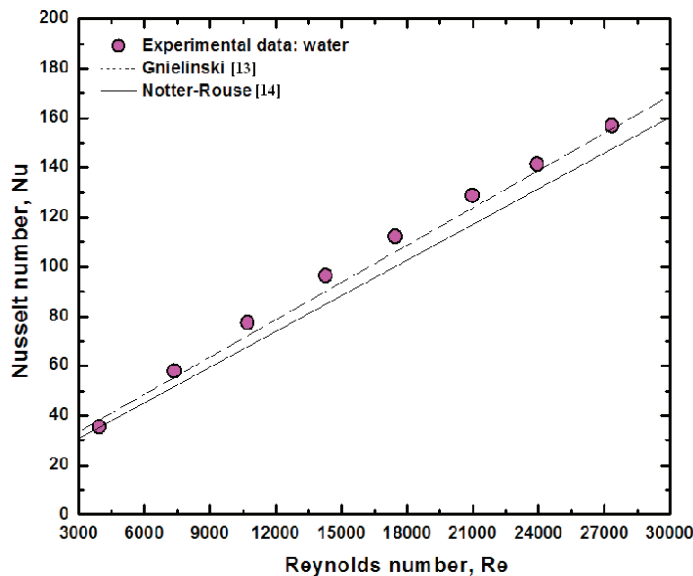


Fig. 2 Validation of experimental Nusselt number of base fluid with the data of Gnielinski (1976) and Notter-Rouse (1972)

Since the fluid flow is fully developed turbulent flow, the friction factor of inlet and outlet pipe is neglected. The friction factor of entire pipes is considered for analysis. Friction factor experiments for water are conducted initially and the values are estimated from Eq. (18). Fig. 3 represents the experimental friction factor of water is in comparison with the data obtained from Eq. (22) of Blasius (1908) and Eq. (23) of Petukov (1970) and found to be a maximum of ±2.5% deviation.

The available friction factor correlations for single phase fluid are given below:

(i) Blasius (1908) equation

$$f = 0.3164 Re^{-0.25} \tag{22}$$

$3000 < Re < 10^5$

(ii) Petukov (1970) equation

$$f = (0.790 \ln(Re) - 1.64)^{-2} \tag{23}$$

$2300 < Re < 5 \times 10^6$

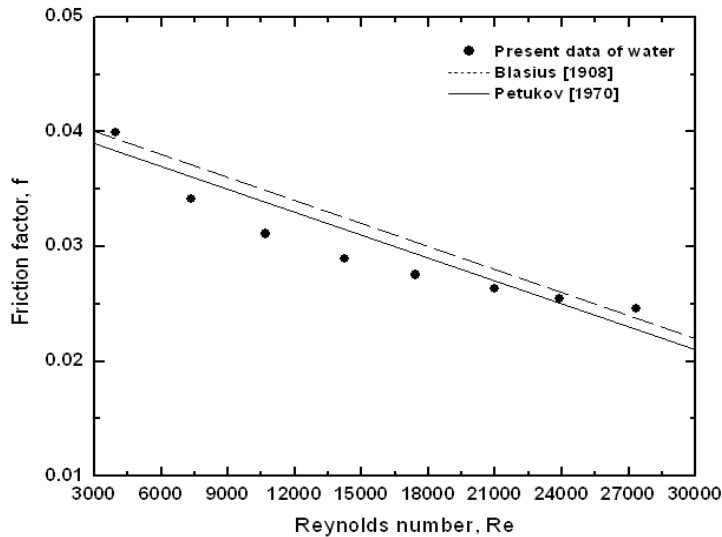


Fig. 3 Validation of friction factor of water compared with Blasius (1908) and Petukov (1970)

4.2 Plain tube without inserts

Heat transfer coefficient in the inner pipe, outer pipe and entire pipe is estimated based on the logarithmic mean temperature distribution. Eq. (16) is used to estimate the Nusselt number and the obtained data for water. It is observed that the Nusselt number in outer pipe is high compared to inner pipe. The Nusselt number enhancement for water is 1.68% at Re = 3000 and 5% at Re = 30000 between inner and outer pipes. This is an example of active method of heat transfer augmentation. The same nature of active method of heat transfer augmentation has been observed by Prabhanjan et al. (2002) and Kumar et al. (2006). Fig. 4 shows the average Nusselt numbers at different Reynolds numbers and concentrations of Al₂O₃ nanofluid in inlet pipe, outlet pipe and entire pipes, respectively. The average Nusselt numbers increase with the rise of the Reynolds number and particle volume concentration. The enhancement of Nusselt number for 0.01% nanofluid at outlet pipe is more than 6.37% compared to the Nusselt number of inlet pipe at a Reynolds number of 30000; whereas for entire pipes, the Nusselt number enhancement is 14.84%. Similarly, the enhancement of Nusselt number for 0.03% nanofluid at outlet pipe is more than 7.2% compared to the Nusselt number of inlet pipe at a Reynolds number of 30000; whereas for entire pipes, the Nusselt

number enhancement is 16.57%.

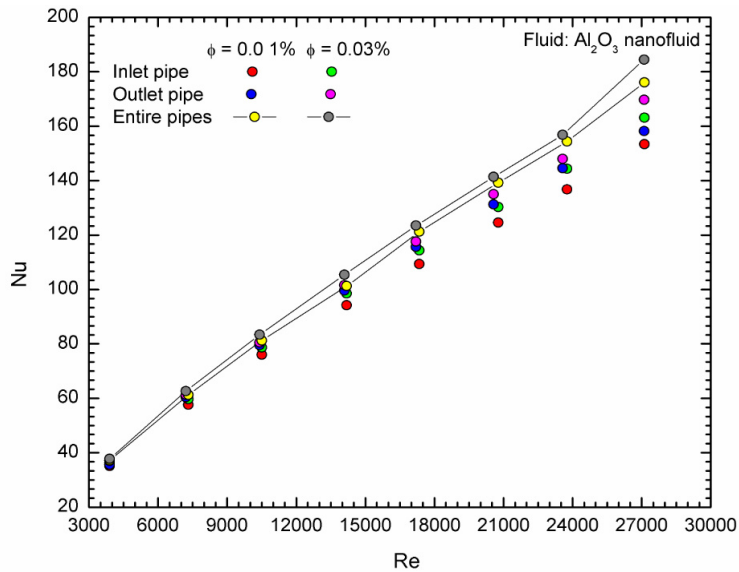


Fig. 4 Comparison of Nusselt numbers of different concentrations of nanofluid in various parts.

The increase in thermal conductivity of nanofluid is a favourite factor for heat transfer enhancement. The trend of nanofluid Nusselt number for entire pipes with 0.01% and 0.03% volume concentration are compared the data with Pak and Cho (1998) and is shown in Fig. 5. The equation of Pak and Cho (1998) under predicts by 7.8% with the present data. Choi and Zhang (2012) have been observed the similar active method of heat transfer augmentation for Al₂O₃ nanofluid in a tube with return bend numerically.

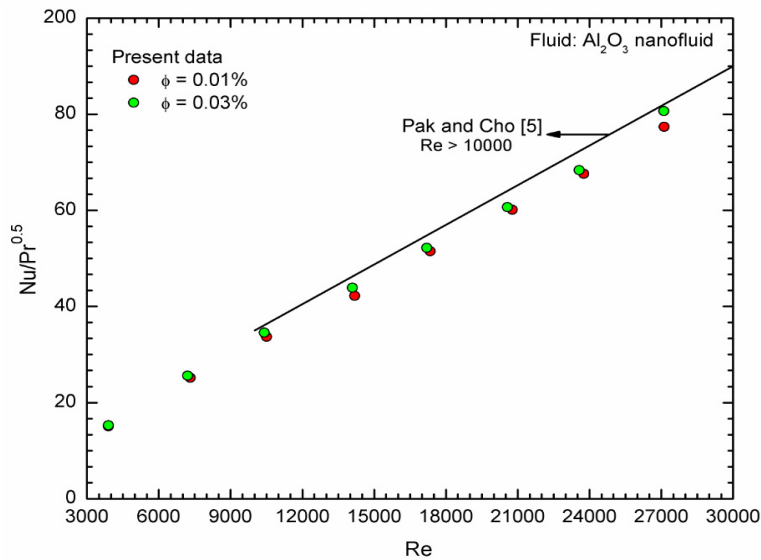


Fig. 5 Nusselt number of 0.01% and 0.03% concentrations of nanofluids estimated at entire pipes is compared with Pak and Cho (1998).

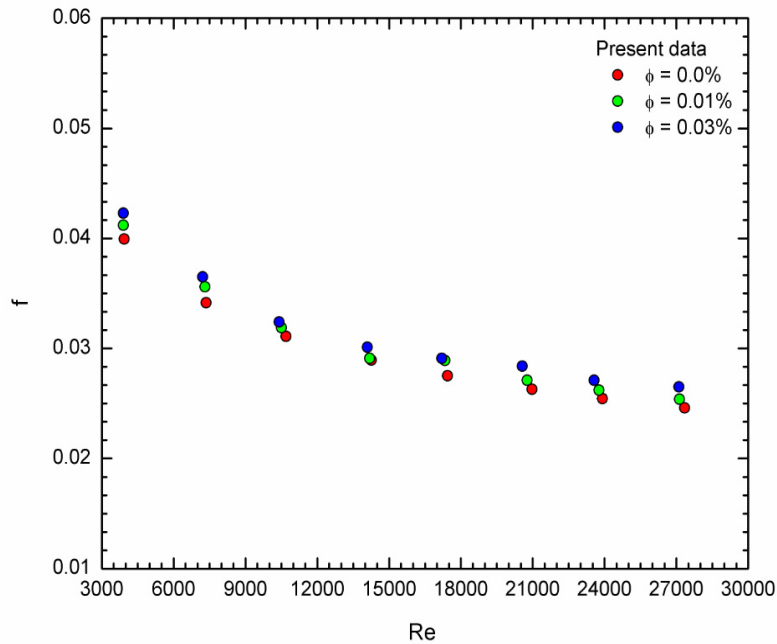


Fig. 6 Comparison of friction factor between 0.01%, 0.03% volume concentration nanofluid and base fluid for entire region.

Experimental friction factor of different volume concentrations of Al_2O_3 nanofluid for entire pipe is estimated from Eq. (17) and is shown in Fig. 6. The friction factor of Al_2O_3 nanofluid increases with increase of Reynolds number and particle concentration. The friction factor of the nanofluid flowing through a tube is purely depends on the flow rate and viscosity. The friction factor enhancement for 0.03% volume concentration of Al_2O_3 nanofluid is about 5.7% and 7.5% at a Reynolds number of 3000 and 30000, respectively compared to water under same flow conditions.

4.3 Effect of trapezoidal – cut in twisted tape on heat transfer augmentation

The heat transfer analysis is also extended to water and nanofluid flowing in a tube with various trapezoidal-cut twisted tape inserts. The Nusselt number of 0.01% and 0.03% volume concentration Al_2O_3 nanofluid with various trapezoidal-cut twisted tape inserts are estimated for entire pipes is shown in Fig. 7. Compared to the same concentration of 0.03% nanofluid in a tube with $H/D = 5$, the Nusselt number enhancement is 15.92% and 24.23% in the Reynolds number of 3000 and 30000, respectively. Compared to the plain tube, the tubes with trapezoidal-cut twisted tapes exhibit higher Nusselt number, because the tape inserts generate swirl flow offering a longer flowing path of fluid flow through the tube and also better fluid mixing, resulting in a thinner thermal boundary layer along the tube wall and thus superior convective heat transfer. Compared to water in a tube and 0.03% nanofluid in a tube with $H/D=5$, the Nusselt number enhancement is 20.69% and 34.24% in the Reynolds number of 3000 and 30000, respectively. This is responsible by the effective fluid mixing by a trapezoidal-cut twisted tape inserts. In addition, the heat transfer enhancement becomes more significant with decreasing the twist ratio of trapezoidal-cut inserts, as the flow area intensity decreases.

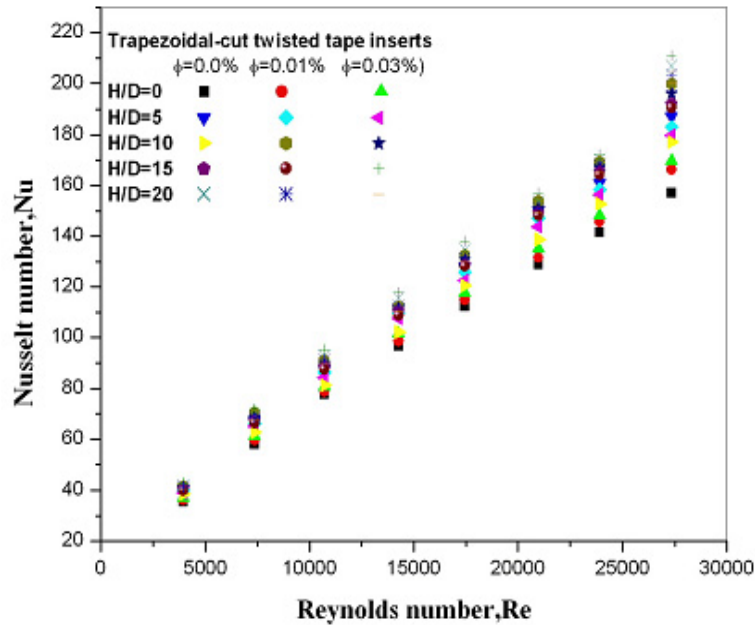


Fig. 7 Experimental Nusselt number Al_2O_3 nanofluid with trapezoidal-cut twisted tape inserts

It can also be observed that the influence of trapezoidal-cut twisted tape inserts on heat transfer is much more significant than that of the presence of nanoparticles in the fluid. The presence of both return bend and trapezoidal-cut twisted tape possibly promotes the dispersion and random movement of the particles, resulting in a better mixing between the core fluid and the tube wall one. Thus the return bend and trapezoidal-cut twisted tapes provide large contact surfaces between fluid and wall which results in the increase of heat transfer.

4.4 Effect of trapezoidal – cut in twisted tape on friction factor.

The data of friction factor for water and nanofluid is shown in Fig. 8. The use of nanoparticles in the base fluid, the friction factor is slightly increased. But this is insignificant penalty in heat transfer enhancement. However, the friction factor of nanofluid increases with increase of Reynolds number and particle concentrations. This can be caused by the increase of shear force on tube wall acted by the larger numbers of nanoparticles. Apparently, the nanofluids with concentrations of 0.03% by volume provide average friction factors higher than the base fluid by around 5.8% and 7.6% in the Reynolds number of 3000 and 30000, respectively. It observed that friction factor increases with increase of Reynolds number, volume concentration and twist ratio of inserts. It is clear that the use of trapezoidal-cut twisted tape results in a very high friction factor than that of plain tube. The friction factor of 0.03% nanofluid flowing in a tube with $H/D=5$ enhances 1.19 times at a Reynolds number of 3000 and 1.29 times at a Reynolds number of 30000 compared to same concentration fluid without trapezoidal-cut twisted tape insert.

The effects of the presence of trapezoidal-cut twisted tape inserts on thermal performance factor are also principally governed by the influence of heat transfer improvement. For the range considered, the maximum thermal performance factor of 1.25 is found with the use of nanofluid of 0.03% by volume in the entire pipes equipped with trapezoidal-cut twisted tape inserts of $H/D = 5$ at Reynolds number of 30000.

5. CONCLUSIONS

The heat transfer and friction factor analysis have been experimentally performed on the water based Al_2O_3 nanofluid in the pipes with return bend and trapezoidal-cut twisted tape inserts. The results show that the average Nusselt numbers increase with an increase of Reynolds number and the nanoparticle volume concentration. Especially, the heat transfer enhancement in the outlet pipes appears larger than the inlet pipes due to the effect of the secondary flow. However, the concentration increment of the nanofluid is accompanied by the high pressure drop in the pipe. Also, the increasing rate of the average Nusselt number is less than that of the thermal conductivity of the nanofluid with the augmentation of the concentration. Under the same Reynolds number, the average Nusselt number of entire pipe for 0.03% concentrations of nanofluid with trapezoidal-cut twisted tape inserts of $H/D = 5$ is enhanced by 34.24% as compared to water. The friction factor of entire pipes for 0.03% concentration of nanofluid with trapezoidal-cut twisted tape inserts of $H/D = 5$ is enhanced by 1.29 times as compared to water. Convective heat transfer, friction factor as well as thermal performance factor associated with the simultaneous application of nanofluid and trapezoidal-cut inserts are higher than those associated with the individual techniques. Convective heat transfer, friction factor as well as thermal performance factor tends to an increase by increasing Al_2O_3 concentration of nanofluid and twist ratio of trapezoidal-cut tape inserts.

6. REFERENCES

- Bergles, A.E., 1995. Techniques to augment heat transfer readings. Handbook of heat transfer applications, New York: McGraw Hill, Chapter 3.
- Blasius, H., 1908. Boundary layers in fluids with small friction, *Z. Math. Phys.*, 56 pp 1-37.
- Chopkar, M., Kumar, S., Bhandari, D.R., Das, P.K., Manna, I., 2007. Development and Characterization of Al_2Cu and Ag_2Al nanoparticles dispersed water and ethylene glycol based nanofluid, *Material science and Engineering B* 139 pp. 141-148.
- Chopkar, M., Das, P.K., Manna, I., 2006. Synthesis and Characterization of nanofluid for advanced heat transfer applications, *Scripta Materialia* 55 pp. 549-552.
- Choi, J. and Zhang, Y. 2012. Numerical simulation of laminar forced convection heat transfer of Al_2O_3 /water nanofluid in a pipe with return bend, *International Journal of Thermal Sciences* 55 pp 90-102.
- Dewan, A., Mahanta, P., Sumithra Raju, K., Suresh Kumar, P., 2004. Review of passive heat transfer augmentation techniques. *J. Power Energy*, Vol. 218, 509–525
- Eastman, J.A., Choi, S.U.S., Li .S., Yu .W., Thompson, L.J., 2001. Anomalous increase in effective thermal conductivity of ethylene glycol-based nanofluids containing copper nanoparticles, *Applied Physics Letters* 78 pp. 718–720.
- Eiamsa-ard, S., Thianpong, C., Promvongse, P., 2006. Experimental Investigation of Heat Transfer and Flow Friction in a Circular Tube Fitted with Regularly Spaced Twisted Tape Elements, *Intl. Communications in Heat and Mass Transfer*, 33, pp.1225-1233.
- Einstein, A., 1956. Investigation on Theory of Brownian Motion, first ed. Dover publications, USA.

- Gnielinski, V., 1976. New equations for heat and mass transfer in turbulent pipe and channel flow, *International Chemical Engineering*. 16 pp 359-368.
- Kumar, V., Saini, S., Sharma, M., Nigam, K.D.P., 2006. Pressure drop and heat transfer study in tube-in-tube helical heat exchanger, *Chemical Engineering Science* 61 pp 4403-4416. New York, (1970) 504-564.
- Lee, S., Choi, S.U.S., Li, S., Eastman, J.A., 1999. Measuring thermal conductivity of fluids containing oxide nanoparticles, *ASME Journal of Heat Transfer* 121 pp.280.
- Maxwell, J.C., 1904. *A treatise on electricity and magnetism*, 2nd Edition, Oxford University Press, Cambridge, UK, 1904.
- Murugesan, P., Mayilsamy, K., Suresh, S., Srinivasan, P.S.S., 2009. Heat transfer and pressure drop characteristics of turbulent flow in a tube fitted with trapezoidal-cut twisted tape insert. *International Journal of Academic Research*, Vol. 1, No.1, pp-123-128.
- Notter, R.H., Rouse, M.W., 1972. A solution to the Graetz problem – III. Fully developed region heat transfer rates, *Chemical Engineering Science* 27 pp 2073–2093.
- Pak, B.C., Cho Y.I. 1998, Hydrodynamic and heat transfer study of dispersed fluids with submicron metallic oxide particles, *Experimental Heat Transfer* 11,pp 151-170.
- Petukhov B.S., 1970. Heat transfer and friction in turbulent pipe flow with variable physical properties, J. P. Hartnett and T. F. Irvine, (Eds), *Advances in Heat Transfer*, Academic Press,
- Prabhanjan, D.G., Raghavan, G.S.V., Rennie, T.J., 2002. Comparison of heat transfer rates between a straight tube heat exchanger and a helically coiled heat exchanger, *International Communications in Heat and Mass Transfer* 29 pp 185-191.
- Wongcharee, K., iamsa-ard, S.,2012. Heat transfer enhancement by using CuO/water nanofluid in corrugated tube equipped with twisted tape, *International Communications in Heat and Mass Transfer* 39, pp 251-257.
- Yadav, A. S., 2008. Experimental investigation of heat transfer performance of double pipe U-bend heat exchanger using full length twisted tape. *International Journal of Applied Engineering Research (IJAER)*, Vol.3, No.3, 399-407.